

REPORT DOCUMENTATION PAGEForm Approved
OMB NO. 0704-0188

Public Reporting burden for this collection of information is estimated to average 1 hour per response, including the time for reviewing instructions, searching existing data sources, gathering and maintaining the data needed, and completing and reviewing the collection of information. Send comment regarding this burden estimate or any other aspect of this collection of information, including suggestions for reducing this burden, to Washington Headquarters Services, Directorate for Information Operations and Reports, 1215 Jefferson Davis Highway, Suite 1204, Arlington, VA 22202-4302, and to the Office of Management and Budget, Paperwork Reduction Project (0704-0188,) Washington, DC 20503.

1. AGENCY USE ONLY (Leave Blank)		2. REPORT DATE 29 March 2005	3. REPORT TYPE AND DATES COVERED Final Progress, 04/15/01 to 12/14/04
4. TITLE AND SUBTITLE Structure Synthesis and Kinetics During undercooled Liquid Solidification and Intense Plastic Deformation		5. FUNDING NUMBERS DAAD 19-01-1-0486	
6. AUTHOR(S) Professor John H. Perepezko			
7. PERFORMING ORGANIZATION NAME(S) AND ADDRESS(ES) University of Wisconsin-Madison Department of Materials Science and Engineering 1509 University Ave. Madison, WI 53706		8. PERFORMING ORGANIZATION REPORT NUMBER	
9. SPONSORING / MONITORING AGENCY NAME(S) AND ADDRESS(ES) U. S. Army Research Office P.O. Box 12211 Research Triangle Park, NC 27709-2211		10. SPONSORING / MONITORING AGENCY REPORT NUMBER 41489.4-ms	
11. SUPPLEMENTARY NOTES The views, opinions and/or findings contained in this report are those of the author(s) and should not be construed as an official Department of the Army position, policy or decision, unless so designated by other documentation.			
12 a. DISTRIBUTION / AVAILABILITY STATEMENT Approved for public release; distribution unlimited.		20050425 024	
13. ABSTRACT (Maximum 200 words) At high undercooling, solidification is rapid and can result in the suppression of the usual reactions to yield amorphous phases and nonequilibrium crystalline phases with novel microstructures. In a complimentary approach, the intense deformation of an elemental layered array drives an atomic scale mixing at the interfaces to yield alloying and in some systems an amorphization reaction. Similarly, deformation of amorphous ribbons can drive instabilities that result in the development of nanocrystal dispersions without annealing. In studies on Al-base amorphous alloys an enhanced control has been achieved for the nanometer-scale microstructure formation processes that operate during primary crystallization. This microstructure is characterized by an ultrahigh number density ($10^{21} - 10^{22} \text{ m}^{-3}$) of Al nanocrystals (20nm in diameter) in an amorphous matrix with a high thermal stability as reflected by a relatively high glass transition temperature, T_g . In order to elucidate the nature of the quenched-in atomic configurations, a novel application of nuclear magnetic resonance and fluctuation microscopy has allowed for the identification of medium range ordered regions that will be analyzed further. A novel strategy to control and enhance the nanocrystal density has been discovered based upon the introduction of nucleants to catalyze nanocrystalline Al. Alternatively, by avoiding quenched-in nuclei through deformation processing, bulk glass formation may be achieved in Al-base alloys. The combination of microcalorimetry and careful size distribution analysis has established the non-steady state nature of primary crystallization. The analysis and modeling of the kinetics is central to devising strategies for reproducible control of primary crystallization including the modification of the crystallization path by exploiting multicomponent diffusion behavior in systems with large differences in component diffusivities. The basic information that the structure synthesis studies yield also has a broad application to many aspects of solidification and deformation processing of ultrafine microstructures. These developments impact other materials treatments such as spray deposition, surface melting, composite fabrication and impact and sliding wear operations and offer a new possibility for novel structure synthesis in bulk volumes.			
14. SUBJECT TERMS Solidification, Nonequilibrium Structure, Metallic Glass, Nanocrystalline Al-Alloys, Multilayer Deformation, Solid-State Amorphization, Crystallization Kinetics, Thermal Analysis, Nucleation			15. NUMBER OF PAGES 19
			16. PRICE CODE
17. SECURITY CLASSIFICATION OR REPORT UNCLASSIFIED	18. SECURITY CLASSIFICATION ON THIS PAGE UNCLASSIFIED	19. SECURITY CLASSIFICATION OF ABSTRACT UNCLASSIFIED	20. LIMITATION OF ABSTRACT UL

MASTER COPY: PLEASE KEEP THIS "MEMORANDUM OF TRANSMITTAL" BLANK FOR REPRODUCTION PURPOSES. WHEN REPORTS ARE GENERATED UNDER THE ARO SPONSORSHIP, FORWARD A COMPLETED COPY OF THIS FORM WITH EACH REPORT SHIPMENT TO THE ARO. THIS WILL ASSURE PROPER IDENTIFICATION. NOT TO BE USED FOR INTERIM PROGRESS REPORTS; SEE PAGE 2 FOR INTERIM PROGRESS REPORT INSTRUCTIONS.

MEMORANDUM OF TRANSMITTAL

U.S. Army Research Office
ATTN: AMSRL-RO-BI (TR)
P.O. Box 12211
Research Triangle Park, NC 27709-2211

☐ Reprint (Orig + 2 copies)

☐ Technical Report (Orig + 2 copies)

☐ Manuscript (1 copy)

☒ Final Progress Report (Orig + 2 copies)

☐ Related Materials, Abstracts, Theses (1 copy)

CONTRACT/GRANT NUMBER: DAAD 19-01-1-0486

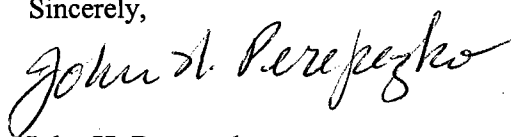
REPORT TITLE: Structure Synthesis and Kinetics During undercooled Liquid Solidification and Intense Plastic Deformation

is forwarded for your information.

SUBMITTED FOR PUBLICATION TO (applicable only if report is manuscript):

DISTRIBUTION STATEMENT A
Approved for Public Release
Distribution Unlimited

Sincerely,



John H. Perepezko

Table of Contents

Scientific Progress and Accomplishments	4 – 12
Figures and Tables	13-16
Publications of the Current Program	17-19
Scientific Personnel	19
References	19

Scientific Progress and Accomplishments

Introduction

In the current program, the research has been focused upon metastable phase formation and the controlling phase selection reactions, the evolution of solidification microstructure in the highly undercooled melts, heterogeneous nucleation sites, characterization of microstructure development and phase stability in metallic glasses, deformation-induced amorphization of multilayers and nanocrystallization in amorphous layers, assessment of thermodynamic properties of amorphous alloys, and several aspects of the kinetics of the formation of metallic glasses. The experimental approaches that have been applied to perform these studies include the droplet emulsification technique, melt-spinning, splat quenching and intense deformation by cold rolling. These methods offer opportunities to produce samples over a wide range of cooling rates and undercooling which could yield various distinct microstructures. In addition, to probe the kinetics of amorphization via solid state reaction and provide the understanding of non-equilibrium processing in depth, cold-rolling has been applied as a means of sample synthesis.

At deep undercoolings equilibrium crystallization reactions may be bypassed and metastable solid phases, including a metallic glass, can be produced during freezing. With thermal analysis and x-ray diffraction experiments it has been possible to examine the undercooling conditions for metastable phase formation and to elucidate the kinetic competition during crystallization. Often the microstructural morphology and the structure of the product phases that solidify from the melt have features that are distinct to high undercooling solidification. For selected reactions it has been possible to identify the solidification path for crystallization from the undercooled liquid state. Based on these findings it has been possible to develop a framework for describing the reaction paths followed during high undercooling solidification in terms of metastable phase diagram constructions. Indeed droplet samples offer a useful method of probing and measuring different portions of metastable phase diagrams.

During the intense deformation that occurs with the repeated cold rolling of multilayer samples it has been established that alloying occurs through an interfacial mixing with elemental multilayers. At high true strain levels the alloying reaction can yield stable and metastable intermediate phases and in some systems an amorphous phase. With multilayers based upon melt spun ribbons of marginal glass forming alloys, intense deformation can yield a nanocrystallization reaction without thermal annealing. A focal point of this portion of the research has been the identification of the proper process and control parameters to describe the deformation driven reactions.

An innovation in experimental capability is the application of microcalorimetry methods to monitor primary crystallization during sub- T_g anneals. By applying microcalorimetry, traditional differential scanning calorimetry (DSC), and transmission electron microscopy (TEM) in the detailed examination of primary crystallization in amorphous an Al-8Sm alloy, the confirmation of the central role of heterogeneous nucleation has been advanced and the transient, non-steady state nature of the reaction has been established for both the nucleation and the growth stages. These central characteristics of the kinetics were identified as a result of the detailed studies involving a combination of microcalorimetry and nanocrystal size distribution measurements. Since the initial structure of melt-spun ribbons is a key to the crystallization kinetics, several collaborative efforts have been pursued to obtain new structural data by NMR, fluctuation microscopy and SAXS measurements. From these efforts it is now evident that the

amorphous structure in melt-spun ribbons contains quenched-in regions of local order that may be the key to control primary crystallization.

Several advances have been made in the understanding of the crystallization behavior and the formation kinetics in amorphous alloys. In the examination of the nucleation mechanism during the primary crystallization of amorphous Al-Y-Fe, the results from numerical modeling have suggested that heterogeneous nucleation is the controlling nucleation mode. In other alloy systems (AlNiY, AlNiCe, FeZrB, FeNbB) where an amorphous phase has been attained by melt-spinning, the crystallization behavior has been characterized by thermal analysis and electron microscopy. A key issue identified in the formation of metallic glasses is the ability to avoid crystallization during rapid quenching. Based upon this, a model describing the kinetics of metallic glass formation by rapid solidification process has been proposed to account for the different thermal responses of the amorphous alloys.

In terms of enhancing materials properties, most Al-base amorphous alloys are effective precursors for synthesizing materials with microstructures consisting of finely dispersed nanocrystalline Al within an amorphous matrix [96FOL, 98INO, 99CAN]. In this regard, nanocrystal density in the Al-Y-Fe amorphous alloy has effectively increased an order of magnitude with the incorporation of small amount of Pb. In addition, it is identified that the key issue in the controlled synthesis of nanocrystalline Al microstructures is the capability to control the nucleation density which appears to be linked to quenched-in features. Advances in understanding the origin of the quenched-in nuclei have been attained with the cross-examination and analysis on the amorphous samples synthesized by melt-spinning and cold-rolling methods. The investigation revealed that these high number density of quenched-in features originated from the rapid quenching process and can be avoided by modifying the reaction pathway. In fact, with cold-rolling of elemental multilayers direct amorphous phase synthesis has been achieved in some systems such as Zr-Al-Cu-Ni and Al-Sm. In other systems, cold-rolling has yielded new insight into the onset of crystallization and the capability of intense deformation to alter the crystallization process.

In the following sections a description is given of the detailed results of the current areas of study. When these findings are viewed together, several new features of the solidification of highly undercooled alloys can be identified from the structure synthesis. The significance and implications of these observations are discussed in terms of the factors determining the rate of solidification, the phase selection process for the solidification products and the microstructural evolution and the new insight on driven system behavior during cold-rolling. A consideration of the results is of value not only in demonstrating the unique potential of the structure synthesis techniques, but also in providing the necessary background for the further development and application of the methods.

Research Highlights

As part of a continuing study of Al alloy systems that offer the potential for the development of large volume fractions of fine dispersoid phases with high temperature stability the current focus has been directed towards amorphous Al-rich Al-Rare Earth Metal (RE)-Transition Metal (TM) alloys and Fe-based alloys. The amorphous Al-RE-TM amorphous alloys have tensile strengths that are comparable to steel and have a lower density than ferrous or titanium alloys. The Fe-based amorphous alloys containing high density of Fe nanocrystals also demonstrate exceptional soft magnetic properties over conventional crystalline magnetic

materials. In order to tailor the microstructure and related properties a clear understanding of the fundamental properties of these Al-rich amorphous alloys is necessary. Extensive work has been reported regarding the compositions and systems that form Al-rich glasses, but these reports provide limited insight into why the Al-RE-TM alloys are relatively easy glass formers, or why these alloys have such relatively high glass transitions [88INO, 93NAK]. In addition, it has been reported that the presence of the Al-nanocrystals increases the tensile strengths observed, but the main variables that affect the formation of the strengthening nanocrystals upon solidification have been limited to wheel speed and alloy composition. Since, the amorphous alloys can decompose to form many different microstructures, an understanding of the reaction kinetics and pathways for microstructure evolution from the initial as-solidified amorphous state is needed. The primary focuses of the current program include the characterization of the metallic glasses, understanding the kinetics of the metallic glass formation, the analysis of the devitrification mechanism, and the catalytic effect of extraneous particles upon crystallization.

Primary Crystallization

Primary crystallization is an important initial reaction during the devitrification of many metallic glasses. For example, in amorphous Al alloys the primary crystallization of a high number density of Al nanocrystals is associated with the attainment of exceptionally high tensile strength values. Experience indicates that the most favorable alloy compositions for Al-base glasses contain 85-92 at.% Al and remaining solute of either rare earth or transition metal components. In spite of the high Al content all of the favored compositions are hypereutectic so that primary phase formation of Al is not favored. Instead, for hypereutectic compositions there is a decided driving free energy advantage to form an intermetallic phase as the primary crystallization product. The observed phase selection points to a heterogeneous nucleation reaction that promotes primary Al nucleation in spite of a driving free energy disadvantage. At the observed number densities of Al nanocrystals the particle separations are of the order of 100nm so that direct examination and identification of potential nucleation sites within the as-quenched amorphous alloy is difficult. There have been several reports where high resolution TEM has indicated the presence of irregular regions that appear to be Al crystallites within an amorphous matrix [i.e. 01GLO, 03KEL, 04WIL], although the identity of a possible precursor heterogeneity has yet to be identified with such electron microscopy techniques. Moreover, kinetics studies have established that the synthesis of the Al nanocrystal dispersion with number densities that exceed 10^{22} m^{-3} is governed by a heterogeneous nucleation process and can increase into the 10^{23} m^{-3} range with minor additions of Cu. At the highest number densities it is difficult to support a conventional heterogeneous nucleation model based upon catalysis by a foreign inclusion and indeed it appears that perhaps some local structural heterogeneity may be the source. Investigations of the initial structure of as-prepared amorphous Al-based alloys, and the thermally and/or mechanically induced microstructural evolution of these alloys, can yield results helpful in identifying the controlling mechanism for formation of microstructures consisting of high densities of Al nanocrystals in marginal Al glass forming alloys.

Isochronal Calorimetry Measurements

Continuous heating calorimetry measurements, following isothermal annealing treatments of various durations at a temperature below the onset of primary crystallization have revealed an experimental limitation in characterizing the primary crystallization behavior of marginal glasses. **Figure 1** indicates that increasing the duration of a pre-crystallization annealing treatment decreases the integrated enthalpy of the resulting primary crystallization exotherm and advances the onset and completion of primary crystallization to higher temperature as measured with continuous heating DSC following a pre-crystallization anneal. A similar result is obtained at other isothermal annealing times and from a comparison based upon percent of α -Al pre-crystallized with the volume fraction transformed during isothermal annealing. Furthermore, as the continuous heating rate (following a given isothermal treatment) is decreased, the integrated primary crystallization enthalpy measured during the subsequent continuous heating scan is decreased relative to that measured at a more rapid heating rate, as seen in **Table 1**. This result indicates that there is a significant amount of crystallization that occurs during continuous heating from room temperature, following the pre-crystallization anneal, to the onset of primary crystallization even though the continuous heating calorimetry baseline (prior to the exothermic crystallization onset) appears to be horizontal (i.e. no measurable heat evolved or absorbed by the sample). This behavior is consistent with thermally activated crystallization and also indicates that the use of continuous heating methods to study primary crystallization behavior is of limited value. In order to investigate the early stages of crystalline phase formation from amorphous precursors, nanocrystallization at low temperatures presents a model case since the slow kinetics enable monitoring the transformation process at high temporal resolution. As a first stage in quantitatively analyzing the early stages of multiple nanocrystal formation, isothermal microcalorimetry experiments have been performed below the glass transition. Therefore, a microcalorimeter has been employed to more accurately measure the heat evolved during the low-temperature annealing treatments. The instrument used here (Thermometric, 2277 TAM) provides a baseline stability better than $0.025 \mu\text{W/h}$, and the temperature of the samples is maintained with an accuracy better than $2 \times 10^{-4} \text{ }^\circ\text{C}$.

Heat Capacity Measurements

The heat capacity of a model binary Al-glass forming composition ($\text{Al}_{92}\text{Sm}_8$, atomic %) was measured over a temperature range of 298 – 1200K on rapidly quenched melt-spun ribbon samples, and slowly quenched droplet samples produced by the salt emulsification technique ($\text{BaCl}_2\text{:CaCl}_2$, 50:50 wt%). Calorimetric measurements in the low-temperature range (298 – 550K) were made on melt-spun ribbon samples in a Perkin Elmer DSC 7 system, while elevated temperature measurements (850 – 1200K) of $\text{Al}_{92}\text{Sm}_8$ droplet samples were conducted with a Netzsch DSC/DTA system. Heating/cooling rates of measurements in both instruments were conducted at 10K/min at ambient pressure in a nominally pure Ar atmosphere. Raw heat flow data of the $\text{Al}_{92}\text{Sm}_8$ droplets ($dQ_{\text{Al-Sm}} / dt$) collected from each instrument was compared to heat flow data of a sapphire standard sample of known heat capacity (dQ_s / dt) to calculate the heat capacity of the crystalline, liquid, and undercooled liquid phases [Eq. 1]; M_s , $M_{\text{Al-Sm}}$, and $C_{p,s}$, $C_{p,\text{Al-Sm}}$ are the respective masses and heat capacities of the sapphire standard and Al-Sm droplet samples.

$$C_{p, Al-8Sm} = \left(\frac{M_s C_{p,s}}{dQ_s/dt} \right) * \left(\frac{dQ_{Al-8Sm}/dt}{M_{Al-8Sm}} \right) \quad (1)$$

The specific heat of the crystalline phase was measured on a heating trace of a previously crystallized melt-spun ribbon slowly cooled to room temperature following a one hour homogenization treatment at 550°C. The specific heat of the crystalline phases shows a linear dependence on temperature as represented by $C_p^{xtal}(T) \approx 7.5 \times 10^{-5} T + 0.65$ J/g-K over the temperature range from 298 – 500K. Initial liquid specific heat measurements on $Al_{92}Sm_8$ droplets, ranging in size from 65-100µm in diameter with an average undercooling of 40K indicate that the specific heat of the undercooled liquid increases with decreasing temperature. The preliminary data can be represented by $C_p^{liq}(T) = -0.0005T + 1.25$ J/g-K. Further measurements to refine the results and extend the undercooling range of measurement by using finer droplet sizes are in progress.

It has been proposed that differences in the specific heat between the metastable undercooled liquid and the equilibrium crystalline phases and the temperature dependence of the configurational entropy are directly related with the change in ΔC_p^{l-xtal} (or slope of configurational entropy as a function of Temperature) being smaller for stronger glass forming systems [95ANG]. The configurational entropy as a function of temperature can be calculated from measured thermodynamic parameters in Eq. 2, where ΔS_c and ΔS_f are the configurational entropy and entropy of fusion, respectively.

$$\Delta S_c = \Delta S_f - \int_T^{T_f} \Delta C_p(T) d \ln T \quad (2)$$

With the availability of a more complete set of specific heat measurements it will be possible to evaluate the configurational entropy and examine the nature of the undercooled liquid behavior in terms of strong and fragile characteristics. The thermodynamic measurements will also provide an essential background for the analysis and interpretation of the results of structural studies concerning the nature of the as-quenched amorphous state.

Al Nanocrystal Development

It is clear from the experimental results that the amorphous structure of the as-quenched alloy plays a vital role in determining its metastability (and subsequent crystallization character). An important result of the current research has been identification of the completely transient nature of the phase transformation in terms of both nucleation and growth. Marginal glass forming alloys have been reported to show a sensitivity to processing and indeed in many cases they illustrate a primary phase that is at a decided disadvantage as the first phase to nucleate in the crystallization scheme. With the usual diagnostic examination for glass formation based upon TEM observation and XRD, marginal glasses appear to represent true amorphous materials. However, it has become increasingly clear that closer examination reveals regions that may possess some ordered arrangements within the amorphous matrix. Small angle scattering and fluctuation microscopy suggest the presence of medium range order. These measurements do not clearly reveal all of the structural features or the chemical environment. Furthermore, some of the measurements are of a local type and do not account for a volume averaged behavior. At the same time, in many glasses, structural relaxation can take place at temperatures in the

vicinity of the glass transition. The relaxation events involve a local densification, and in some cases a change in chemical short range ordering as well. This has not been explored fully in the case of the marginal glass forming alloys although some relaxation response would be expected. Moreover, it is evident that any clustering or local structural change may represent a small volume of the sample and will require a high sensitivity and resolution for detection. In this regard nuclear magnetic resonance (NMR) offers an attractive option with a high sensitivity to local chemical environment and a capability of identifying different environments for a given component.

SAXS

Small-angle scattering of x-rays (SAXS) represents a fundamental method for structure analysis of condensed matter. The scattering of x-rays at small angles (close to the primary beam) provides structural information on inhomogeneities of the electron density with characteristic dimensions between one and a few hundred nm. For the current research program, SAXS experiments provide the opportunity to sample the size distributions of particles whose sizes remain below the resolution of conventional electron microscopy techniques (< 5 nm diam). SAXS measurements will be conducted at the Argonne National Laboratory Advanced Photon Source in collaboration with Professor Paul Evans at the University of Wisconsin-Madison.

An initial SAXS investigation of partially vitrified amorphous Al-Sm ribbons annealed at 130°C for 3 and 6 hours has been performed. **Figure 2a** shows the particle size distributions obtained for Al-Sm amorphous melt spun ribbons annealed for 3 and 6 hours respectively. As shown in these results, the first three hours of annealing accounts for three times the nucleation events that occurs in the second three hours. This is a clear indication that the nucleation rate is decreasing and is unfit for analysis using conventional steady-state nucleation theory. Further, the negligible difference in average size and the range in crystal size indicates that the relevant growth kinetics affect crystals approximately 12 nm in diameter and smaller. The subsequent shifting of the crystal size distributions to larger values reflects dendritic growth, which represents a second growth mechanism. From a statistical standpoint, using small angle scattering to measure size distributions will allow particles beyond the capabilities of conventional TEM treatments to be resolved, resulting in a higher measured particle density- as shown in **fig. 2b**.

Compared to particle counting analysis of TEM micrographs, a more robust statistical analysis of data acquired from SAXS can be obtained due to the fact that SAXS is a volume averaging technique whereas TEM only probes a small 2-D slice of the microstructure. The SAXS technique provides confirmatory measurements that allow us to efficiently probe the evolving structure of marginal glasses at a large number of times and temperatures.

Fluctuational Microscopy

Nucleation sites for primary crystallization in melt-spun $\text{Al}_{92}\text{Sm}_8$ metallic glass may be a form of nanometer length scale structural order, or medium-range order (MRO). Understanding the nature of this structure and how processing can modify it will be important to tailoring the devitrification of high Al-content metallic glass. The potential for deviations from a dense random packed structure in real metallic glass samples is also of significant fundamental interest.

Fluctuation electron microscopy (FEM) is a technique to quantitatively detect MRO in amorphous materials [96TRE, 00VOY]. FEM uses hollow-cone dark field imaging in a transmission electron microscope (TEM) to measure diffraction from nanoscale volumes of the sample. As the electron beam is tilted, pockets of structural order will meet a Bragg condition and strongly scatter electrons; an excited Bragg condition will generate a bright spot in a dark field micrograph compared to the amorphous matrix. If there are more ordered regions in the sample (more MRO), there will be more bright spots in the image. If the beam is tilted between Bragg conditions, the ordered pockets will appear particularly dark. Overall, the more speckle of bright and dark areas that appear in a dark field micrograph, the more MRO is present in the sample. The specific size of MRO clusters measured by the FEM method is dependent upon the size of the objective aperture in place in the TEM [00VOY]. At present, the spatial resolution limit (governed by the electron microscopy equipment available at UW-Madison) of the FEM technique is 16Å.

FEM investigations on amorphous $\text{Al}_{92}\text{Sm}_8$ prepared by melt-spinning and cold-rolling of elemental foils have shown distinct differences in type and degree of medium range order (MRO) in the amorphous phase (**Fig. 3**) suggesting that the MRO may be a precursor to primary crystallization, thus differentiating the crystallization mechanism in amorphous samples prepared by different processing routes [04STR].

Nuclear magnetic resonance spectroscopy

Collaborative efforts with Professor Yue Wu at the University of North Carolina, utilizing NMR to probe the evolution of the primary phase, are currently underway. For Al base systems NMR is a particularly sensitive and effective probe of local atomic configurations. While previous thermal analysis and electron microscopy studies do not indicate quantitative differences in the amorphous "structure" of as-solidified ribbon samples due to subtle differences in processing conditions during melt spinning, the NMR measurements reported here are the first to provide direct proof of differences in the as-solidified sample volume of two independent batches of $\text{Al}_{92}\text{Sm}_8$ MSR. In order to establish a basis for comparison, the observations on melt spun amorphous ribbons are analyzed from two separate processing runs that were conducted to be replicate runs. For this purpose, in addition to processing the identical alloy chemistry (i.e. $\text{Al}_{92}\text{Sm}_8$), the key melt spinning process parameters such as wheel speed (55m/s), melt superheat and duration, gas ejection pressure and nozzle size were controlled to be as identical as is possible. The resulting ribbons had a similar appearance and dimensions. As revealed in **figure 4a**, the x-ray diffraction patterns from the two samples were also essentially identical and indicate that they are macroscopically amorphous. Other common diagnostic measures such as TEM examination (BF and SAD) and DSC examination that are shown in **figure 4b** provide further evidence that the two samples are amorphous and in terms of the usual structural and thermal behavior for the onset of primary crystallization are essentially identical.

As solidified MSR samples were annealed for various times at 130°C to induce crystallization of primary Al nanocrystals in the residual amorphous matrix. Subsequently, nuclear-magnetic-resonance (NMR) measurements were performed on the as-solidified and annealed ribbon specimens. Details regarding the NMR experimental procedure and results analysis can be found elsewhere [00WUc]. While XRD, thermal analysis, and electron microscopy studies do not indicate quantitative differences in the microstructure of as-solidified ribbon samples due to subtle differences in processing conditions during melt spinning, the NMR

spectra from the two independent specimens show a clear and quantitative difference. Based upon a comparison with the Knight shift signal from pure crystalline Al both sample A and B display a noticeable amount of Al in a crystalline environment as well as the majority of Al in less well-defined amorphous environment.

NMR scans (measured with identical pulse sequences) of ribbon samples from "Batch A" and "Batch B" (both batches of ribbon prepared by melt spinning with a peripheral wheel speed of 55m/s) show a broad signal peaking at a Knight shift position slightly higher than that of pure Al coupled with the presence of a small peak at the Knight shift position corresponding to pure Al [figure 5]. However, the relative magnitude of the Al peak is distinctly different between the two sample batches, indicating that different volume fractions of each sample exist in a specific local atomic configuration corresponding to clusters of pure Al atoms. The broad shoulder in the NMR data sets at higher Knight shift positions than Al corresponds to the Al-rich amorphous phase in the as-solidified samples. Quantum mechanical analyses of NMR measurements on the two independent as-solidified MSR batches show that the volume percentage of aluminum in the amorphous matrix, clustered into a specific local atomic environment representative of crystalline Al, ranges from 3 – 5 vol% in separate sample batches. From this analysis it is apparent that amorphous Al alloys are indeed sensitive to processing conditions. Even in a given laboratory and when processing is replicated as much as possible, there is a notable difference in the as-quenched condition of the samples. For comparison, an NMR scan of a MSR sample from "batch A" that was annealed at 130°C for 10hr. shows a more intense Al peak than wither of the as-solidified samples indicating that a large volume fraction of Al clusters (or nanocrystals) is present in the matrix.

Based on these measurements, and assuming that the as-solidified amorphous matrix contains some volume fraction of spherical primary Al clusters (ranging from 3 – 20 vol%) acting as potential heterogeneous nucleation sites, the number of Al clusters was calculated as a function of possible cluster size with possible cluster size ranging from 0.2 – 1nm [figure 6a]. Subsequently, a normal distribution of cluster sizes was calculated assuming a mean cluster diameter of 0.5nm for an amorphous Al-Sm matrix containing 3 and 5 vol% Al atoms in spherical clusters. Integration of the normal distribution results indicates that 1.1×10^{21} and 1.8×10^{21} clusters of Al atoms ranging from 0.35 – 0.65nm in diameter (within +/- one standard deviation (σ) of the mean (η)) would exist in the amorphous matrix assuming 3% and 5% volume fraction transformed respectively [figure 6b].

Summary

From the progress and results that have been achieved during the current program, several aspects of solidification and amorphization under high undercooling conditions and deformation-induced transitions have emerged as new behavior that impacts the understanding of nanostructured evolution. One area of central interest is the early stage evolution of nanocrystals that is essential to developing a clear understanding of the controlling nucleation and growth kinetics. The initial findings in the current research indicate that a non steady state growth rate, that may reflect concurrent relaxation, contributes to the reaction, which will require further experiments to quantify and model. It seems highly probable that the source of the transformation kinetics behavior stems from the as quenched state. Structural and calorimetric analyses have been applied in the current work to understand the as-quenched state of the amorphous sample, and to quantify the effect of quenched in features on the primary phase

nanocrystallization kinetics. The overarching goal is to identify a means to process – through thermal, chemical, or mechanical treatments – as-quenched marginal glasses so as to achieve a reproducible initial state for the material in order to allow for prediction of the evolution of primary phase nanocrystals based upon a given driving force. Towards this goal the insight into structure synthesis behavior provided by critical experiments and systematic structure characterization have been used to initiate the development of kinetics analysis models for phase selection and microstructure evolution.

Figures

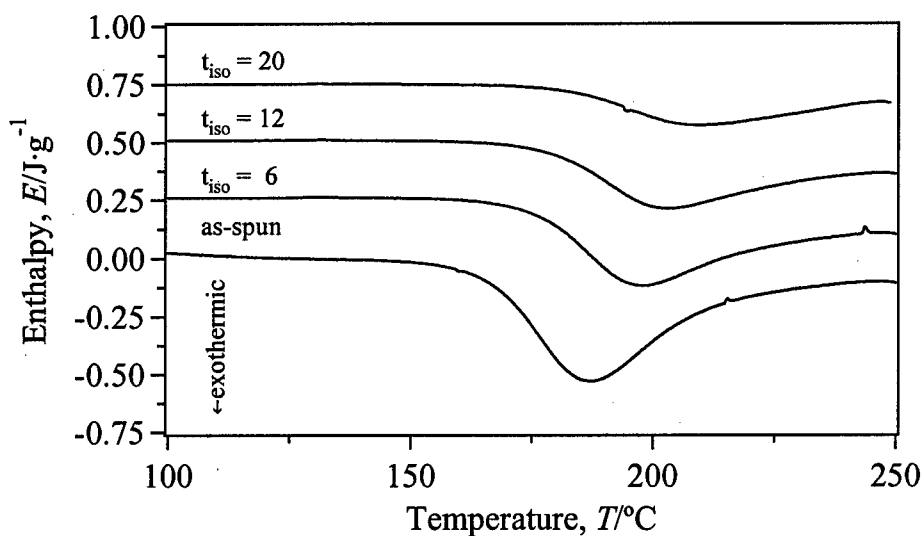


Figure 1. Continuous heating DSC traces at 20K/min of amorphous $\text{Al}_{92}\text{Sm}_8$ MSR after pre-annealing at 130°C for varying times.

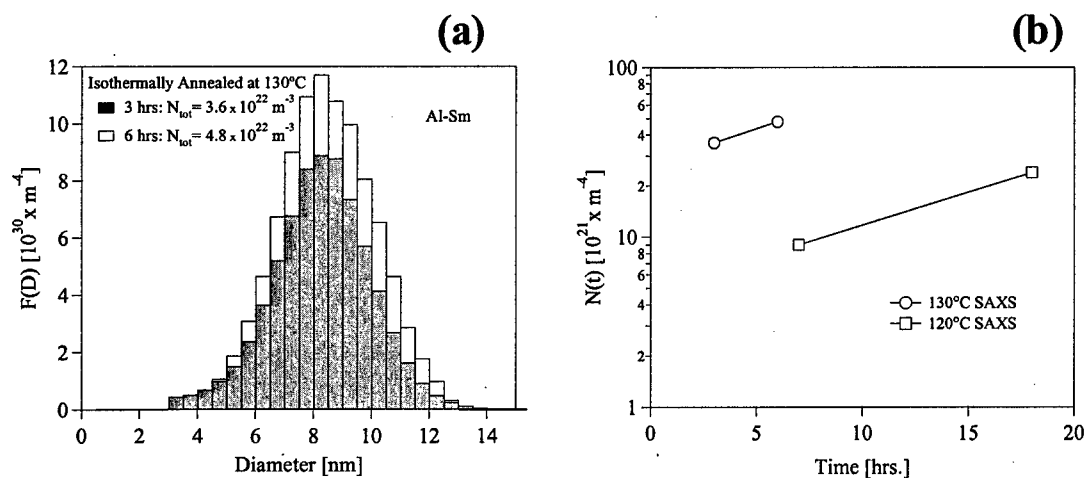


Figure 2. (a) Particle size distributions obtained for Al-Sm amorphous melt spun ribbons annealed for 3 and 6 hours respectively. (b) measured number densities, N , measured from SAXS at 120° and 130° for different annealing times and different analysis methods.

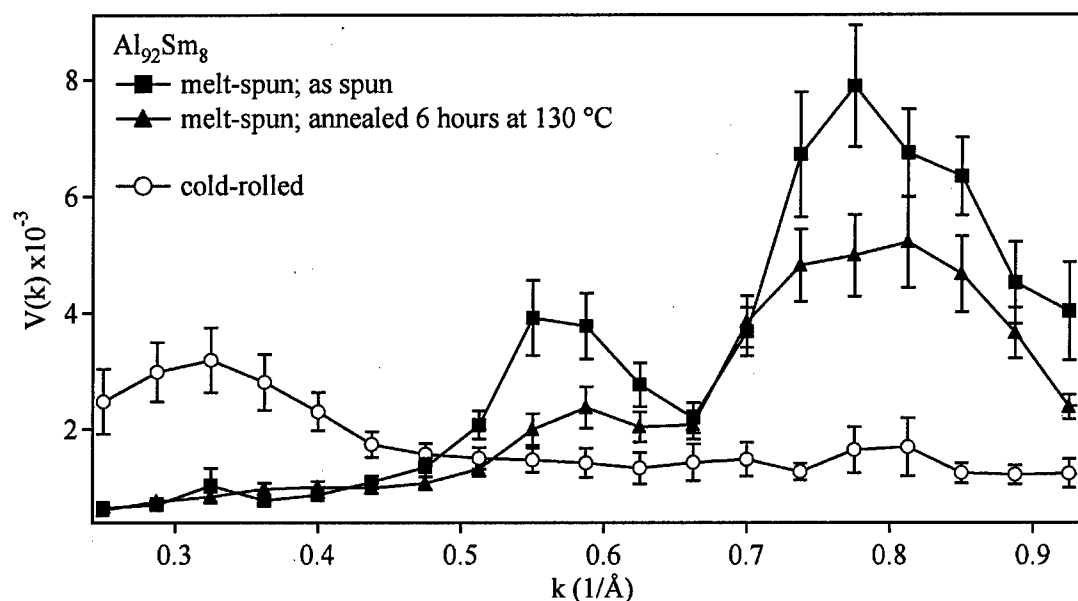


Figure 3: $V(k)$ for melt-spun as-spun, melt-spun annealed, and cold-rolled $\text{Al}_{92}\text{Sm}_8$ metallic glass. The peak locations in the as-spun and annealed samples are the same, showing that the same type of MRO is present in both samples. The height of the peaks decreases, indicating a decrease in the degree of MRO. The cold-rolled samples shows a lower peak in a different location, indicating it has less MRO of a different type than the either melt-spun sample.

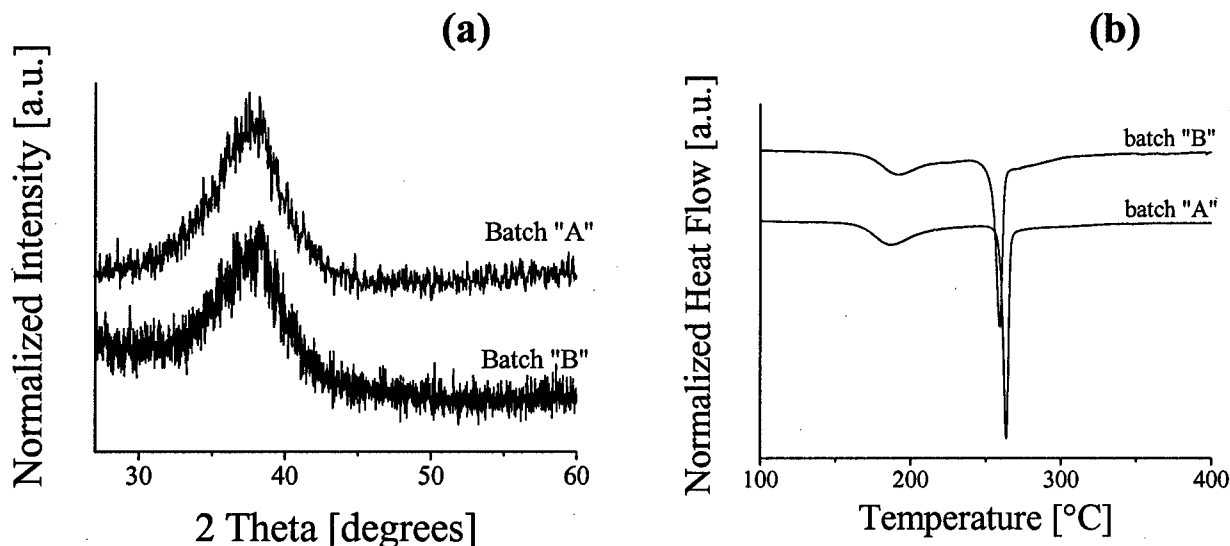


Figure 4: (a) XRD traces of replicate batches of $\text{Al}_{92}\text{Sm}_8$ MSR samples prepared at 55m/s. (b) continuous heating DSC traces ($dT/dt = 20^\circ\text{C}/\text{min}$) of replicate batches of $\text{Al}_{92}\text{Sm}_8$ MSR

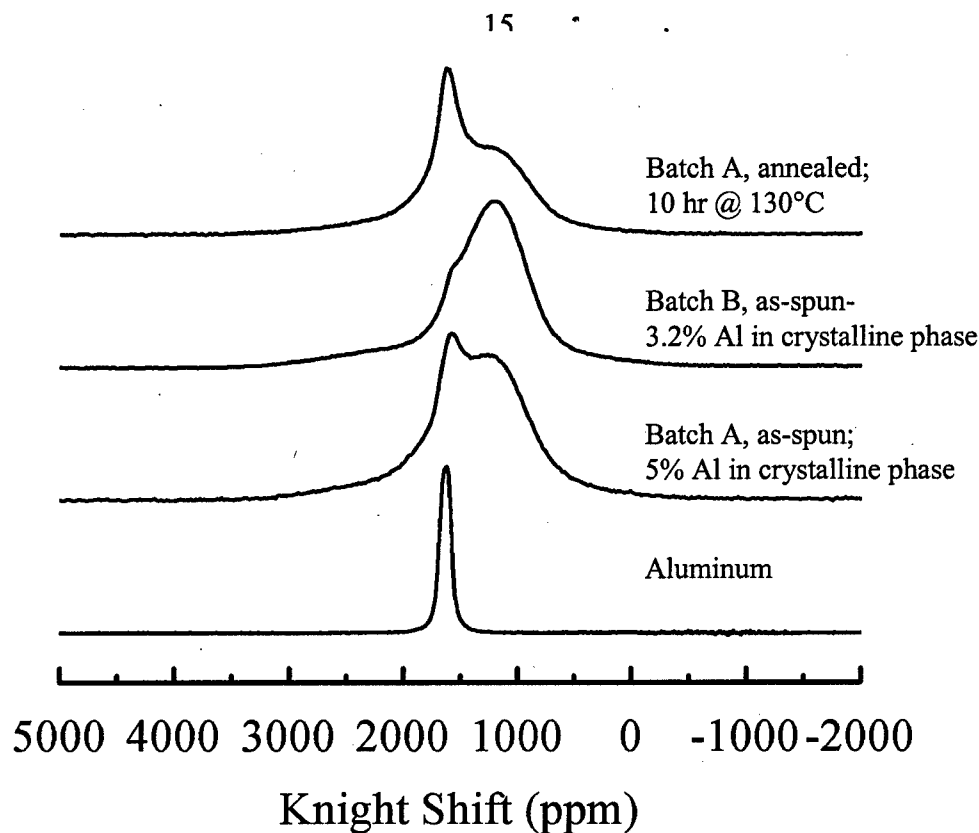


Figure 5: NMR traces of pure Al and replicate batches of as-spun and annealed $\text{Al}_{92}\text{Sm}_8$ MSR

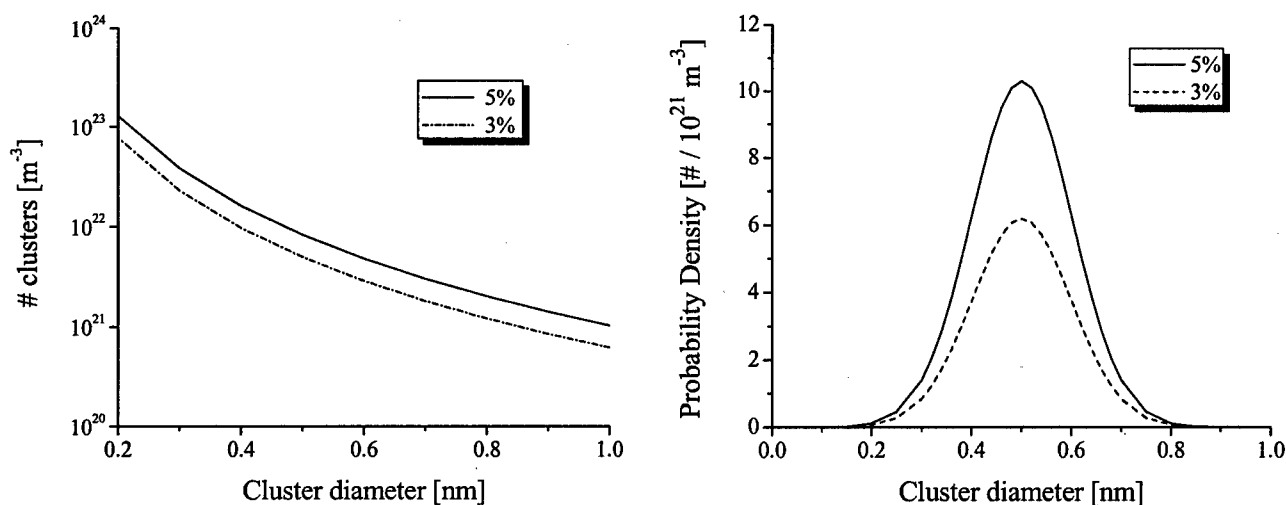


Figure 6: (a) calculated number of Al clusters of a given diameter that could possibly fill 3 – 5% volume fraction of the matrix. (b) normal distribution $[N(\mu, \sigma)]$ of Al cluster sizes assuming 3 vol% and 5vol% of the matrix is occupied by clusters of Al atoms

Table 1

Isothermal Annealing time 130°C [hours]	Continuous Heating DSC @ 10 K/min			Continuous Heating DSC @ 20 K/min			Isothermal Micro- calorimetry	Microstructural Examination
	Onset T_{α} [°C]	$\Delta H_{\alpha-Al}$ [J/g]	Percent α -Al pre- crystallized [†]	Onset T_{α} [°C]	$\Delta H_{\alpha-Al}$ [J/g]	Percent α -Al pre- crystallized [†]	Measured Enthalpy [J/g]	Volume Fraction [%]
0	161	73	0	165	61	0	0	0
6	167	52	9	175	54	4	4	0.5
12	171	42	14	178	44	10	6.5	0.9
20	174	29	21	182	25	20	9	n/a

Publications of the Current Program

During a research program, substantial time intervals often elapse between the completion of a research study, submission of a manuscript and the final appearance of a paper in print. As a result, the following list gives publications in preparation as well as those in print or in press. (The papers noted by an asterisk are invited). Interim reports for this grant were submitted to the ARO in 2002, 2003, and 2004.

1. "Solid State Amorphization by Cold Rolling", H. Sieber, G. Wilde, A. Sagel and J. H. Perepezko, EUROMAT 2000, Materials Development and Processing-Bulk Amorphous Materials, Undercooling and Powder Metallurgy, 8, 3, (2000).
2. "Intermetallic Phase Formation in Bulk Multilayered Structures", H. Sieber and J. H. Perepezko, EUROMAT 2000, Intermetallics and Superalloys, 10, 324, (2000).
3. "Nucleation Kinetics Analysis by Repeated Solidification of Single Droplets", G. Wilde, J. Sebright, P. Hockel and J. H. Perepezko, EUROMAT 2000, Materials Development and Processing-Bulk Amorphous Materials, Undercooling and Powder Metallurgy, 8, 85, (2000).
4. "Superheating" J.H. Perpezko, The Encyclopedia of Mat. Sci. and Technology, Eds. K.H.J. Buschow, R.W. Cahn, M.C. Flemmings, B. Ilshner, E.J. Kramer, and S. Mahajan, Elsevier (Oxford), 8975, (2001).
5. "Low temperature, mercury-mediated synthesis of aluminum inetmetallics", M. Khoudiakov, A. B. Ellis, J. H. Perepezko, S. Kim and K. D. Kepler, Chemistry of Materials, 12, 2008-2013 (2000).
6. "Amorphization and alloy metastability in under-cooled systems", J. H. Perepezko and G. Wilde, J. Non-Cryst. Solids, 274, 271-281 (2000).
7. "Kinetics of glass formation and nanocrystallization in Al-RE-(TM) alloys", R. I. Wu, G. Wilde and J. H. Perepezko, Minerals, Metals and Materials Society/AIME, Ultrafine Grained Materials, p63-72, (2000).
8. " Cold-rolling of Al-based alloys ", R. J. Hebert, G. Wilde, H. Seiber and J. H. Perpezko, Minerals, Metals and Materials Society/AIME, Ultrafine Grained Materials, 165-172, (2000).
9. "Liquidus and temperature determination in multicomponent alloys by thermal analysis", R. I. Wu and J. H. Perepezko, Met. Mat. Trans., 31A, 497-501 (2000).
10. "Glass formation and nanostructure development in Al-based alloys", R. I. Wu, G. Wilde, and J. H. Perpezko, Mat. Res. Soc. Symp., Vol, 101-106 (2000).
11. "Nanostructure formation by rapid solidification and solid state processing", R. I. Wu, R. J. Hebert and J. H. Perepezko, ASM International, Understanding Processing, Structure, Property, and Behavior Correlations, 27, 12, (2000).
12. "Glass formation and primary nanocrystallization in Al-base metallic glasses", J. H. Perepezko, R. I. Wu, and G. Wilde, Mat. Sci. & Engr. A., 301, 12-17 (2001).
13. "Undercooling and glass formation in Al-based alloys", S. K. Das, J. H. Perepezko, R. I. Wu and G. Wilde, Mat. Sci. & Engr. A, **304-306**, 159-165, (2001).
14. "Synthesis and stability of amorphous Al alloys", J. H. Perepezko, R. I. Wu, R. Hebert and G. Wilde, Mat. Res. Soc. Symp. (2001)
15. "Amorphous aluminum alloys- synthesis and stability" J. H. Perepezko and R. J. Hebert, JOM, 54, 34-39 (2002).

16. "The significance of the heat of mixing for the amorphization of multilayers by deformation processing" R. J. Hebert and J. H. Perepezko, *Materials Science Forum*, **386-388**, 21-26 (2002).
17. "Nanostructure synthesis and amorphization during cold rolling", J. H. Perepezko, R. J. Hebert and R. I. Wu, *Materials Science Forum*, **386-388**, 11-20 (2002).
18. "Heterogeneous microstructural evolution and reaction during repeated intense deformation", R. J. Hebert and J. H. Perepezko, *Ultrafine Grained Materials II*, Eds. Y.T. Zhu, T.G. Langdon, R.S. Mishra, S.L. Semiatin, M.J. Saran, and T.C. Lowe (TMS, Warrendale, PA), 141, (2002).
19. "Initial crystallization kinetics in undercooled droplets", J. H. Perepezko, P. G. Hockel and J. S. Paik, *Thermochimica Acta*, **388**, 129-141 (2002).
20. "Amorphization and nanostructure synthesis in Al alloys" J. H. Perepezko, R. J. Hebert and W. S. Tong, *Intermetallics*, **10**, 1079-1088 (2002).
21. "Undercooling and solidification of atomized liquid droplets", J. H. Perepezko, J. L. Sebright, P. O. Hockel and G. Wilde, *Mat. Sci. & Engr. A*, **326**, 144-153, (2002).
22. "Solidification of atomized liquid droplets", J. H. Perepezko, J. L. Sebright and G. Wilde, *Adv. Engr. Mat.*, **4**, 147-151, (2002).
23. "Primary crystallization in amorphous Al-based alloys", J. H. Perepezko, R. J. Hebert, R. I. Wu, and G. Wilde, *Journal of Non-Crystalline Solids*, **317**, 52-61 (2003).
24. "Nucleation-catalysis-kinetics analysis under dynamic conditions", J. H. Perepezko and W. S. Tong, *Philosophical Transactions of the Royal Society of London Series A*, **361**, 447-460 (2003).
25. "Nanocrystallization in Al-rich metallic glasses", G. Wilde, N. Boucharat, R. J. Hebert, H. Rösner, W. S. Tong and J. H. Perepezko, *Advanced Engineering Materials*, **5**, 125-130 (2003).
26. "Nanometer-scale solute clustering in aluminum-nickel-ytterbium metallic glasses", D. Isheim, D. N. Seidman, J. H. Perepezko, G. B. Olson, *Materials Science and Engineering A*, **353**, 99-104 (2003).
27. "Structural transformations in crystalline and amorphous multilayer samples during cold-rolling", R. J. Hebert and J. H. Perepezko, *Scripta Mat.*, **49**, 933-939 (2003).
28. "Nanocrystallization Reactions in Amorphous Aluminum Alloys", J. H. Perepezko, R. J. Hebert, W. S. Tong, J. Hamann, H. R. Rösner and G. Wilde: *Mater. Trans. JIM* **44**, 1982-1993 (2003).
29. "Deformation-induced crystallization and amorphization of Al-based metallic glasses", R. J. Hebert and J. H. Perepezko, *Mat. Res. Soc. Symp.*, **754**, 267-272 (2003).
30. "Analysis of primary crystallization in amorphous aluminum alloys", J. H. Perepezko, W. S. Tong, J. Hamann, R. J. Hebert, H. R. Rösner and G. Wilde, *Mat. Res. Soc. Symp. Proc.*, **754**, 347-352 (2003).
31. "Deformation-induced synthesis and structural transformations of metallic multilayers", R. J. Hebert and J. H. Perepezko, *Scripta Materialia*, **50**, 807-812 (2004).
32. "Nucleation-controlled reactions and metastable structures," J. H. Perepezko, *Progress in Materials Science*, **49**, 263-284 (2004).
33. "Thermally Controlled Nanocrystallization in Amorphous Al Alloys", J. Hamann, W. S. Tong, H. Rösner, J. H. Perepezko and G. Wilde, *Solid State Phenomena*, **101-102**, 259-264 (2005).

34. "Medium-Range Order in High Al-content Amorphous Alloys Measured by Fluctuation Electron Microscopy", W.G. Stratton, J. Hamann, J.H. Perepezko, P.M. Voyles, *Mat. Res. Soc. Symp. Proc.*, **806**, 275-280 (2004).
35. "Early stages of Al-nanocrystal formation in $\text{Al}_{92}\text{Sm}_8$ ", G. Wilde, H. Rösner, J. Hamann, W.S. Tong, J.H. Perepezko, *Mat. Res. Soc. Symp. Proc.*, **806**, 33-38 (2004).
36. "Primary Nanocrystallization and Amorphous Alloy Stability", J. H. Perepezko, R. J. Hebert, *J. Non-Equilib. Processing*, *accepted*.
37. "Deformation-induced mixing reactions in Cu-Cd multilayers", R. J. Hebert, G. Wilde, J. H. Perepezko, *J. Non-Equilib. Processing*, *accepted*.

Scientific Personnel

Professor John H. Perepezko, Principal Investigator
 Robert Wu, Ph.D conferred 2001
 Rainer Hebert, Ph.D conferred 2003
 Joseph Hamann, M.S. conferred 2003
 Dr. William Scott Tong-Postdoctoral Fellow (partial support)
 Undergraduate students – R. Birringer and J. Karel

References

- [88INO] A. Inoue, K. Ohtera, A. P. Tsai, and T. Masumoto, *Jpn. J. Appl. Phys.*, **27**, L280, (1988).
- [93NAK] K. Nakazato, Y. Kawamura, A.P. Tsai, A. Inoue, *Appl. Phys. Lett.*, **63**, 2644, (1993).
- [95ANG] C. A. Angell, *Science*, **267**, 1924, (1995).
- [96FOL] J. C. Foley, D. R. Allen, J. H. Perepezko, *J. Non-Cryst. Solids*, **207**, 559, (1996).
- [96TRE] M. M. J. Treacy and J. M. Gibson, *Acta Cryst. A* **52**, 212 (1996).
- [98INO] A. Inoue, H. Kimura, and L. Wang, *Mat. Trans. JIM*, **39**, 866, (1998).
- [99CAN] B. Cantor, *Mat. Sci. Forum*, **307**, 143, (1999).
- [00VOY] P. M. Voyles, J. M. Gibson, and M. M. J. Treacy, *J. Electron Microsc.* **49**, 259 (2000).
- [01GLO] T. Gloriant, D. H. Ping, K. Hono, A. L. Greer, M. D. Baró, *Mat. Sci. & Eng. A304-306*, 315, (2001).
- [03KEL] K. F. Kelton, T. K. Croat, A. K. Gangopadhyay, L.-Q. Xing, A. L. Greer, M. Weyland, X. Li, K. Rajan, *J. Non-Cryst. Solids*, **317**, 71, (2003).
- [04STR] W.G. Stratton, J. Hamann, J.H. Perepezko, P.M. Voyles, *Mat. Res. Soc. Symp. Proc.*, **806**, 275, (2004).
- [04WIL] G. Wilde, H. Rösner, J. Hamann, W. S. Tong, J. H. Perepezko, *Mat. Res. Soc. Symp. Proc.*, **806**, 33, (2004).